Biophysical *Journal*
Article

Biophysical Society

Computational model of E-cadherin clustering under force

Yang Chen,[1,2] Julia Brasch,[3] Oliver J. Harrison,[3] and Tamara C. Bidone[1,2,*]
[1]Department of Biomedical Engineering, [2]Scientific Computing and Imaging Institute, and [3]Department of Biochemistry, University of Utah, Salt Lake City, Utah

ABSTRACT E-cadherins play a critical role in the formation of cell-cell adhesions for several physiological functions, including tissue development, repair, and homeostasis. The formation of clusters of E-cadherins involves extracellular adhesive (*trans*-) and lateral (*cis*-) associations between E-cadherin ectodomains and stabilization through intracellular binding to the actomyosin cytoskeleton. This binding provides force to the adhesion and is required for mechanotransduction. However, the exact role of cytoskeletal force on the clustering of E-cadherins is not well understood. To gain insights into this mechanism, we developed a computational model based on Brownian dynamics. In the model, E-cadherins transit between structural and functional states; they are able to bind and unbind other E-cadherins on the same and/or opposite cell(s) through *trans*- and *cis*-interactions while also creating dynamic links with the actomyosin cytoskeleton. Our results show that actomyosin force governs the fraction of E-cadherins in clusters and the size and number of clusters. For low forces (below 10 pN), a large number of small E-cadherin clusters form with less than five E-cadherins each. At higher forces, the probability of forming fewer but larger clusters increases. These findings support the idea that force reinforces cell-cell adhesions, which is consistent with differences in cluster size previously observed between apical and lateral junctions of epithelial tissues.

SIGNIFICANCE Tissue repair and maintenance are regulated by adhesions between cells. To establish their function, cell-cell adhesion proteins sense and transmit mechanical force, but exactly how force affects their dynamics is largely unknown. Here, we develop the first, to our knowledge, computational model of cell-cell adhesion assembly based on force-dependent mechanisms. The model shows that force promotes the assembly of large clusters. By contrast, without force, only small puncta of adhesion proteins emerge. Our results reconcile a number of previous observations reporting differences in cell-cell adhesion size and density in various conditions.

INTRODUCTION

Physical connections between cells mediated by E-cadherins support the development of all soft tissues, facilitate cell sorting during morphogenesis, and govern wound healing and collective cell migrations (1–4). Misregulation of the adhesive functions of E-cadherins can result in loss of cell-cell adhesions, epithelial-mesenchymal transition, reduced tissue permeability, and metastatic initiation, a hallmark of cancerous cells (5,6). Understanding how cells form and maintain clusters of E-cadherins in cell-cell adhesion can help elucidate the biophysical mechanisms underlying tissue development and repair and may lead to future treatments for cancer cell invasion.

E-cadherins are single-pass transmembrane glycoproteins that form both *trans*-associations between ectodomains of opposed E-cadherins and lateral *cis*-interactions between E-cadherins on the same cell surface (Fig. 1 *A*) (7–11). The intracellular domain of E-cadherin is linked to the contractile actomyosin cytoskeleton beneath the cell membrane through the catenin complex, which becomes active after the formation of E-cadherin lateral interactions (12–15).

The formation of cell-cell adhesions is a multistep process, in which E-cadherins dynamically transit between molecular states from free monomers to *trans*-dimers (Fig. 1 *A*), clusters of E-cadherins, and interactions with the actomyosin cytoskeleton. *Trans*-dimerization of E-cadherins is mediated by the membrane-distal extracellular cadherin (EC) subunits EC1 and EC2 and involves at least two distinct structural states: first, a short-lived X-dimer forms from monomers,

Submitted May 14, 2021, and accepted for publication October 18, 2021.
*Correspondence: tamarabidone@sci.utah.edu
Julia Brasch and Oliver J. Harrison contributed equally to this work.
Editor: Pablo Iglesias.
https://doi.org/10.1016/j.bpj.2021.10.018

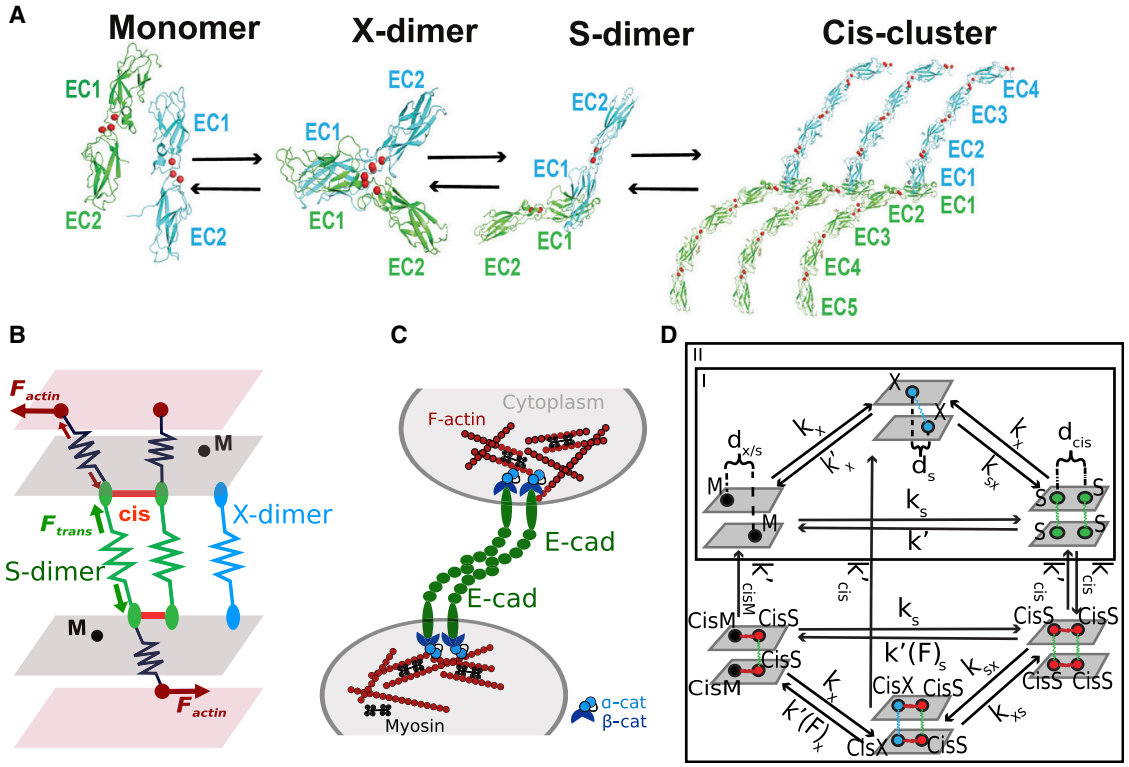

FIGURE 1 Computational model incorporates E-cadherin transitions across molecular state. (*A*) E-cadherin monomers from opposed cell membranes (ribbon representation of two monomers in *green* and *blue*, respectively; Protein Data Bank (PDB): 1Q1P) associate via an "X-dimer" interface (PDB: 3LND) to form a mature strand-swapped dimer, "S-dimer" (only EC1–2 are shown for clarity; PDB: 3Q2V). Multiple S-dimers form a *cis*-cluster through adhesive (*trans*-) and lateral (*cis*-) interactions (ribbon representation of the extracellular domains of E-cadherins in *cis*-cluster: EC1-5 lattice crystal structure; PDB: 3Q2V). (*B*) Schematic illustration of the 3D computational domain, with two inner surfaces representing the membranes of neighboring cells and two outer surfaces representing the actomyosin cytoskeleton. E-cadherins within cell membranes are represented as beads, undergoing transitions in molecular states: free monomers (in *black*), X-dimers (*blue*), S-dimers (*green*), and *cis*-clusters (*red*). The actin cytoskeleton binding sites are represented as particles on the external surface, exerting force F_{actin} with a probability *P*. (*C*) Graphical representation of the molecular elements involved in force-transmission across E-cadherins. (*D*) The inner rectangle (*I*) indicates the kinetic map for E-cadherins transitions between molecular states in force-free conditions. Freely diffusing monomers, M, form fast intermediate X-dimers (rate constant k_x) to then stabilize into S-dimers (rate constant k_{sx}) or form S-dimers directly (rate constant k_s). S-dimers can form *cis*-interactions (rate constant k_{cis}). Corresponding backward rate constants are indicated as k_x', k_x, k_s', and k_{cis}'. The outer rectangle (*II*) illustrates the implemented kinetic map in conditions of simulated cytoskeletal force. The bottom triangle shows that E-cadherins in the cluster can transit between CisM, CisX, and CisS (counterparts of M, X, and S when in the *cis*-cluster) according to forward and backward rates or even return to M, X, and S if no *cis*-interaction is formed. To see this figure in color, go online.

which can then convert into a final and more stable strand-swapped S-dimer (Fig. 1 *A*) (16–18). S-dimers can cluster by establishing lateral *cis*-interactions mediated by EC1-EC2 (Fig. 1 *A*) (14,15,19,20) and connection to the actin cytoskeleton through activation of the catenin complex (13,14). These transitions across molecular states also proceed backward, with disassembly of *cis*-interactions and transitions from S- to X-dimers and monomers (17,21).

Cell-cell adhesions show differences in the size of E-cadherin clusters and in their number per unit area of cell membrane (20,22–24). These differences have been attributed to varying surface concentrations of E-cadherins (25), their mobility and adhesive properties (26), their association with the actomyosin cytoskeleton, and the local spatial arrangement of actin filaments and bundles (24).

E-cadherins sense and transmit cellular force to support tissue remodeling and homeostasis (13,27,28). Cytoskeletal force is transferred to E-cadherin through α- and β-catenin; if E-cadherin is bound to an opposite E-cadherin, then cytoskeletal force is transmitted across the X or S *trans*-dimer (Fig. 1, *B* and *C*). Under force, the lifetime of the trans-dimer varies: the X-dimer behaves as a catch-slip bond and stabilizes up to ~30 pN (Fig. S1 *A*); the S-dimer behaves as a slip bond, with decreasing bond lifetime under increasing force (Fig. S1 *A*); and when the S-dimer converts to an X-dimer, the lifetime of the *trans*-interaction is insensitive to force (29,30). On the intracellular side, E-cadherins are connected to the catenin complex, which forms a two-state catch bond with the actin cytoskeleton with force-dependent transitions between the weakly and strongly bound states (Fig. S1, *B* and *C*) (13).

Although it has been established that actomyosin force regulates interactions between E-cadherins and with the actomyosin cytoskeleton, exactly how force mediates their

TABLE 1 Parameters used in the model of E-cadherin clustering

Parameters	Description	Values	References
k_x	forward rate constant of binding from M + M to X	3.8×10^4 s^{-1}	(31)
k_x'	backward rate constant of unbinding from X to M + M	1.84×10^3 s^{-1}	(31)
k_s	forward rate constant of binding from M + M to S	0.31 s^{-1}	(31)
k_s'	backward rate constant of unbinding from S to M + M	1.27×10^{-4} s^{-1}	(31)
k_{xs}	forward rate constant of binding from X to S	86 s^{-1}	(31)
k_{sx}	backward rate constant of unbinding from S	0.86 s^{-1}	(31)
k_{cis}	forward rate constant of *cis* binding from S to *cis*	100 s^{-1}	(31)
k_{cis}'	backward rate constant of unbinding CisX and CisS to X and S	0.1 s^{-1}	(31)
k_{cisM}'	backward rate constant of unbinding from CisM to M	100 s^{-1}	estimated
D	2D diffusion coefficient of cadherin	28×10^{-3} $\mu m^2/s$	(23)
d_x	cutoff distance to form X from M + M	3 nm	estimated
d_s	cutoff distance to form S from M + M or X	1 nm	(31)
d_{cis}	cutoff distance to form *cis* from S	8 nm	(24)
Δt	time step	10^{-5} s	estimated

N/A, not applicable.

clustering remains elusive. A detailed and quantitative understanding of how force affects E-cadherin clustering has been hindered by a lack of experimental approaches able to simultaneously detect changes in the molecular state of individual E-cadherins and differences in the dynamics of clustering from multiple E-cadherins. Previous models analyzed the formation of clusters of E-cadherins based on transition rates, but they did not consider force-dependent mechanisms (31,32). In this study, we developed the first, to our knowledge, computational model of E-cadherin clustering under force and tested the hypothesis that force-dependent transitions across E-cadherin molecular states affect cluster size and their density per unit area. Our new, to our knowledge, findings provide a picture in which force can tune the structural and dynamic properties of E-cadherin clusters by delaying their assembly and increasing their size.

MATERIALS AND METHODS

To understand the multistep process of E-cadherin clustering under force, we developed a mesoscale model incorporating transitions between E-cadherin molecular states (Fig. 1 *A*). In the model, two parallel surfaces represent the two parallel membranes of neighboring cells, where individual E-cadherins are exemplified as single-point particles (Fig. 1 *B*) that diffuse in Brownian motion (diffusion coefficient $D = 0.028$ $\mu m^2/s$, from (24)). The two simulated cell membranes are separated by 20 nm, a dimension of the same order as that observed in electron micrographs of adherens junctions and desmosomes (33). Assembly and disassembly of E-cadherin dimers and their lateral clustering and connections with the cytoskeleton are based on a kinetic scheme (summarized in Fig. 1 *D*). The actin cytoskeleton is represented as two external surfaces, where "ghost" particles appear at a given probability, *P*, to bind and pull E-cadherins by exerting force, $\boldsymbol{F_{actin}}$, parallel to the cell membrane. This force is then transmitted across the *trans*-dimer as $\boldsymbol{F_{trans}}$, through an elastic interaction (Fig. 1 *B*). Simulations start with a random distribution of free E-cadherin monomers on the two internal surfaces. Then, E-cadherin monomers freely diffuse and transit across molecular states, including formation of X- and S-dimers, lateral *cis*-interactions, and connection with the actin cytoskeleton. Once clustered and connected to the actomyosin cytoskeleton, $\boldsymbol{F_{actin}}$ is exerted on them. In particular, $\boldsymbol{F_{actin}}$ is first distributed on all E-cadherins that are bound to the actomyosin cytoskeleton, then to all E-cadherins in the same cluster. This mimics the linkage between multiple catenin complexes in a cluster with the same actin bundle through a multitude of anchors (34,35).

We run two sets of simulations in different force conditions: force free (Fig. 1 *D I*) and with force (Fig. 1 *D II*). In force-free conditions, forward and backward rate constants for *trans*-dimerization and formation of *cis*-associations between E-cadherins were based on experimentally determined binding affinities (20,36), similar to (31). When force was used, the backward rate constants were estimated based on lifetime versus force relations (Fig. S1) from single-molecule traction force and optical tweezers experiments (13,29,37). Because E-cadherin monomers can also exist in the *cis*-cluster (38) but are less stable than X- or S-dimers in the cluster (because of the lack of the *trans*-binding), a larger backward rate constant was used for monomers in clusters with respect to X- or S-dimers (Table 1).

Brownian dynamics simulations

The Langevin equation was used to simulate the two-dimensional (2D) motion of each E-cadherin, *i*, in the limit of high friction:

$$\boldsymbol{F_i} - \varepsilon_i \frac{d\boldsymbol{r_i}}{dt} + \boldsymbol{F_i^T} = 0\,, \tag{1}$$

where $\boldsymbol{r_i}$ is a position vector of the *i*-th E-cadherin, ε_i is a drag coefficient corresponding to the 2D diffusion coefficient $D = 0.028$ $\mu m^2/s$ (24), dt is simulation time step of 10^{-5} s, and $\boldsymbol{F_i}$ and $\boldsymbol{F_i^T}$ are deterministic and stochastic forces acting on the *i*-th E-cadherin, respectively.

The deterministic force acting on each *i*-th E-cadherin results from the actomyosin force, $\boldsymbol{F_{actin}}$, and the force from the *trans*-interaction, $\boldsymbol{F_{trans}}$:

$$\boldsymbol{F_i} = \boldsymbol{F_{actin}} + \boldsymbol{F_{trans}} \tag{2}$$

The force from the actomyosin cytoskeleton has a direction parallel to the simulated cell membranes and displaces E-cadherins laterally because their vertical motion is restrained by the friction of the cell membrane. Upon E-cadherin displacement, force is then transmitted to the *trans*-dimer and thus to the opposite E-cadherin, which also moves laterally. Therefore, E-cadherins on both cell membranes respond to cytoskeletal and *trans*-dimer forces through lateral movement.

Cytoskeletal force was systematically varied in our simulations according to a defined probability, *P*, which determines the probability by which an actin bead appears (as a "ghost" bead) to bind E-cadherins in clusters. Cytoskeletal force varied within the range 10–50 pN, corresponding to physiological values of actomyosin force acting on E-cadherins in cells and to the range estimated for E-cadherin binding strength from single-molecule experiments (13,39,40).

Forces from interactions with the actin cytoskeleton follows Hooke's law, as

$$\boldsymbol{F_{actin}} = k_{actin}(l - l_{actin,0}) , \quad (3)$$

with spring constants $k_{act} = 2$ pN/μm and equilibrium separations $l_{actin,0} =$ 10 nm, of the order of cell membrane thickness (41).

Forces from *trans*-interactions between E-cadherins also follows Hooke's law as

$$\boldsymbol{F_{trans}} = k_{trans}(l - l_{trans,0}) , \quad (4)$$

with spring constants $k_{trans} = 2$ pN/μm and equilibrium separations $l_{trans,0} = 20$ nm, characteristic of adhesive separation between E-cadherins (8,20).

The stochastic force represents the effect of thermal fluctuations generating Brownian motion and diffusive behavior of E-cadherins. This force satisfies the fluctuation-dissipation theorem (42) as

$$\boldsymbol{F_i^T}(t)\boldsymbol{F_j^T}(t) = \frac{2k_BT\varepsilon_i\delta_{ij}}{\mathrm{d}t}\boldsymbol{\delta} , \quad (5)$$

where k_B is the Boltzmann constant, T is the temperature, δ_{ij} is the Kronecker δ, and $\boldsymbol{\delta}$ is a unit second-order tensor. Our model assumes that monomers and X- and S-dimers diffuse, whereas clusters are stationary. Because of the higher entropy of X-dimers relative to S-dimers, each E-cadherin forming an X-dimer is subjected to a stochastic Brownian force that is independent from the force acting on the other. In this molecular state, the two E-cadherins are subjected to thermal forces that differ for magnitude and direction but maintain their harmonic connection. By contrast, E-cadherins forming an S-dimer diffuse together, and the stochastic force is applied with the same magnitude and direction on both monomers of the dimer.

The positions of E-cadherins are updated at every time step of the simulations using explicit Euler integration scheme:

$$\boldsymbol{r_i}(t + dt) = \boldsymbol{r_i}(t) + \frac{d\boldsymbol{r_i}}{dt}dt = \boldsymbol{r_i}(t) + \frac{\boldsymbol{F_i^T} + \boldsymbol{F_i}}{\varepsilon_i}dt \quad (6)$$

Kinetic interactions between E-cadherins in force-free conditions

The kinetic map proposed by (31) is first implemented to simulate *trans*-dimerization and clustering of E-cadherins in the absence of actomyosin force (Fig. 1 *D I*). Initially, an equal number of E-cadherins in the state of monomers (M) is randomly distributed on each simulated cell membrane. By implementing the overdamped Langevin equation (Eq. 1) to simulate Brownian motion, free diffusion of E-cadherin monomers on the opposite membranes occurs. When two monomers from opposite membranes come in proximity, meaning that they reach a distance closer than $d_x = 3$ nm, they can either form a fast intermediate X-dimer (X) at a rate k_x or, if closer than $d_s = 1$ nm, directly form an S-dimer at a rate k_s. If they form an X-dimer (X), this molecular state can further stabilize into a strand-swapped S-dimer (S) at a rate k_{sx}. Because the formation of *trans*-dimers effectively reduces the entropy for lateral binding of E-cadherins (24), the model assumes that *trans*-dimerization is followed by formation of lateral *cis*-interactions (15,19), depending on distance (threshold separation is $d_{cis} = 8$ nm) and forward rate k_{cis} (Table 1). In the absence of cytoskeletal force, each forward transition is associated with a fixed backward transition and therefore a backward rate (Table 1). To evaluate the likelihood of a forward or backward transition, the corresponding probability is evaluated as

$$p_{\substack{on\\off}} = k_{\substack{on\\off}} \times dt \quad (7)$$

Kinetic interactions between E-cadherins under force

When force is used, the backward rate constants of the E-cadherin *trans*-interactions depend on the magnitude of the force acting on the *trans*-dimer (37). Force-dependent unbinding kinetics of X-dimers follows a catch-bond model (Fig. S1 *A*), with the unbinding rate versus force relation as

$$k_{off} = 100\, e^{\frac{-0.34\ \boldsymbol{F_{trans}}}{4.114}} + 0.7\, e^{\frac{0.34\ \boldsymbol{F_{trans}}}{4.114}} \quad (8)$$

Force-dependent unbinding kinetics of S-dimers follows a slip-bond model (Fig. S1 *A*), with unbinding rate versus force relation as

$$k_{off} = 1.27E - 4\, e^{0.0819\ \boldsymbol{F_{trans}}} \quad (9)$$

These lifetime versus force relations for catch and slip bonds are used to determine unbinding rates and corresponding probabilities of state transitions from dimers to monomers. Once a dimer dissociates into two monomers, it can still exist as clustered E-cadherins if the lateral interactions still exist. The fact that our model assumes that E-cadherin monomers, X-dimers, and S-dimers can coexist within the same cluster means that *trans*- and *cis*-interactions are independent from one another, as previously detected experimentally (15,43). The kinetic map allowing *trans*-dimerization of E-cadherins from monomers within the cluster is shown in an inverted triangle in Fig. 1 *D II*. Monomers or dimers can leave the cluster, depending on the backward rate constant for lateral interactions (Table 1).

Interactions between E-cadherins and the actin cytoskeleton

Because E-cadherins can interact with the actomyosin cytoskeleton underneath the plasma membrane, our model assumes that E-cadherins can bind the actomyosin cytoskeleton on the external surfaces of the three-dimensional (3D) domain (Fig. 1 *B*). In cells, this link is created through activated α-catenins at a late stage of cell-cell adhesion nucleation and E-cadherin clustering (14,15,44). Therefore, in the model, binding between actin and E-cadherin occurs when E-cadherins are involved in *cis*-interactions. Additionally, this binding occurs based on a defined probability, P, that accounts for the possibility of actin networks with different architectures and differences in motor activity (45–47). Binding between actin and E-cadherin occurs by establishing a harmonic interaction with stiffness 2 pN/μm and equilibrium separation 10 nm, a dimension comparable to membrane thickness (48). Force is applied on the actin bead on the external surface of the model after interaction with E-cadherin, in a direction parallel to the simulated cell membrane. This force builds tension on the actin-E-cadherin connection and modulates unbinding. Unbinding of E-cadherin from actin follows a two-state catch-bond model with weakly and strongly bound states and dynamic transitions between them (Fig. S1, *B* and *C*), as previously reported (13). The strongly bound state is expressed as a function of the force on the bond, $\boldsymbol{F}$:

$$k_{off} = e^{\frac{-2\ \boldsymbol{F}}{4.114}} + 3E - 4\, e^{\frac{2\ \boldsymbol{F}}{4.114}} \quad (10)$$

The weakly bound state is expressed as a function of the force acting on the bond, $\boldsymbol{F}$:

$$k_{off} = 5e^{\frac{-2\ \boldsymbol{F}}{4.114}} + 3E - 3\, e^{\frac{2\ \boldsymbol{F}}{4.114}} \quad (11)$$

Transitions from the weakly to strongly bound state have a rate of

$$k_{w/s} = 3e^{\frac{0.2\ \boldsymbol{F}}{4.114}} \quad (12)$$

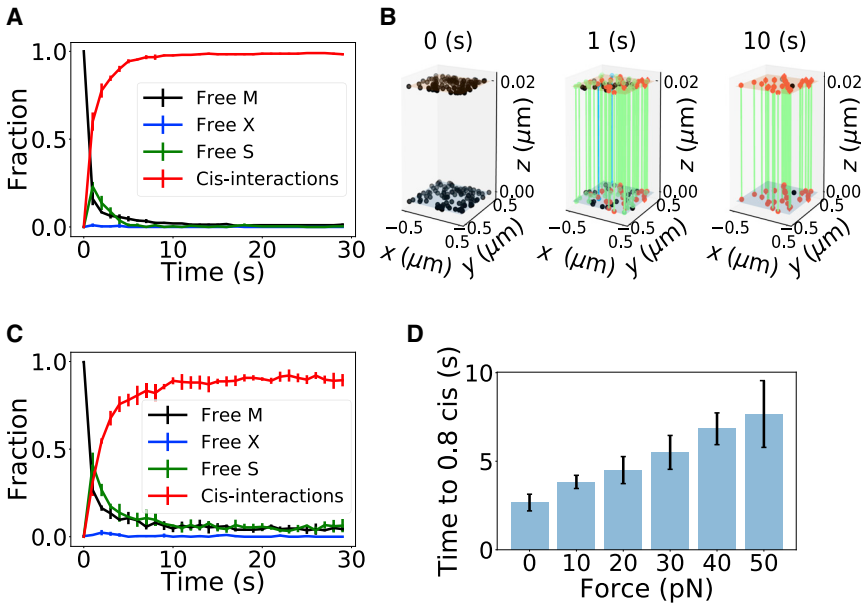

FIGURE 2 Force reduces the fraction of E-cadherins in *cis*-interactions. (*A*) Average fraction of the different molecular states of E-cadherins in force-free conditions. The different lines indicate free monomers M (*black*), free X- (*green*) and S- (*blue*) dimers, and *cis*-interactions (*red*). Data are computed from three independent simulations using 100 E-cadherins on each cell membrane. Error bars indicate standard deviations from the mean. (*B*) Snapshots of E-cadherin states and positions at the beginning of the simulations (0 s), at the beginning of clustering (1 s), and when steady state is reached (10 s). E-cadherins are single-point particles represented in different colors, depending on their molecular state: black, monomers; blue, free X-dimers; green, free S-dimers; and red, E-cadherins in *cis*-interactions. Connections between E-cadherins in opposite cell membranes are shown in different colors depending on their molecular state: blue, X-dimers, and green, S-dimers. (*C*) Average fraction of E-cadherins in different molecular states under 30 pN force. The different lines indicate free monomers, M (*black*); free X- (*green*) and S- (*blue*) dimers; and *cis*-interactions (*red*). Data are computed from three independent simulations using 100 E-cadherins per cell membrane. Error bars indicate standard deviations from the mean. (*D*) Average time at which a fraction of 0.8 E-cadherins becomes involved in *cis*-interactions for forces between 10 and 50 pN. Data are computed from six independent simulations. Error bars indicate the standard deviation from the mean. To see this figure in color, go online.

Transitions from the strongly to weakly bound state have a rate of

$$k_{s/w} = 20e^{\frac{-4F}{4.114}} \quad (13)$$

RESULTS

Force delays the incorporation of E-cadherins into clusters

During clustering, the fractions of free monomers (M) and X-and S-dimers and the fraction of E-cadherins involved in *cis*-interactions varied depending on force conditions. In force-free conditions, within the first 5 s of simulations, the fraction of free monomers decreased from 1 to less than 0.1 and the fraction of E-cadherins involved in *cis*-interactions increased from 0 to more than 0.9 (Fig. 2 *A*). In particular, within the first 1 s of simulations, formation of free S-dimers from monomers occurred, corresponding to an increase of the fraction of free S-dimers from 0 to ~0.2. Then, free S-dimers were incorporated into clusters, and thus, their fraction decreased below 0.1, whereas the fraction of E-cadherins involved in *cis*-interactions reached steady state (Fig. 2 *A*). Consistently, 3D snapshots of the simulations showed that starting from free monomers distributed on the two simulated cell membranes, a few X-dimers were formed at 1 s that become S-dimers and are incorporated into clusters at 10 s (Fig. 2 *B*).

Using $F_{actin} = 30$ pN, similar trends were observed in the fractions of each E-cadherin molecular state, with monomers decreasing rapidly and free S-dimers increasing and then decreasing as they were incorporated into clusters. The fraction of E-cadherins incorporated into *cis*-interactions increased with time (Fig. 2 *C*). However, in contrast to the force-free conditions, differences in the proportions of each molecular state and the time taken to establish steady state were observed. Whereas free monomers decreased as observed in the force-free conditions (Fig. 1 *A*), the proportion of free monomers did not reach near zero under force, instead reaching a steady state of 0.045 ± 0.016 (Fig. 2 *C*). Free S-dimers initially increased to a higher fraction, 0.41 ± 0.07 (Fig. 2 *C*), than in force-free conditions (Fig. 2 *A*) before declining as they were stably incorporated into clusters. Free S-dimers also presented a steady state not near zero, as in force-free conditions, but at 0.05 ± 0.018 (Fig. 2 *C*). In both force-free and force-dependent conditions, free X-dimers were below 0.05 at steady state. More detailed analysis of the fractions of the different molecular species of E-cadherins at higher time resolution showed that a fraction of X-dimers larger than 0.1 formed from monomers within 0.1 s of simulations, both without and with force (Fig. S2, *A* and *B*). This fraction decreased to a steady state below 0.05 within 1 s. In particular, the time needed to plateau was around 0.2 s without force and around 0.4 s with force (Fig. S2, *C* and *D*). This result indicates that the X-dimer molecular state was short-lived and transient, consistent with (15), and also affected by force.

To understand why force changes the proportions of E-cadherins in the different molecular states, we systematically varied its magnitude and evaluated the time it takes to reach more than a fraction of 0.8 E-cadherins in *cis*-interactions. Our results showed a direct proportion between force

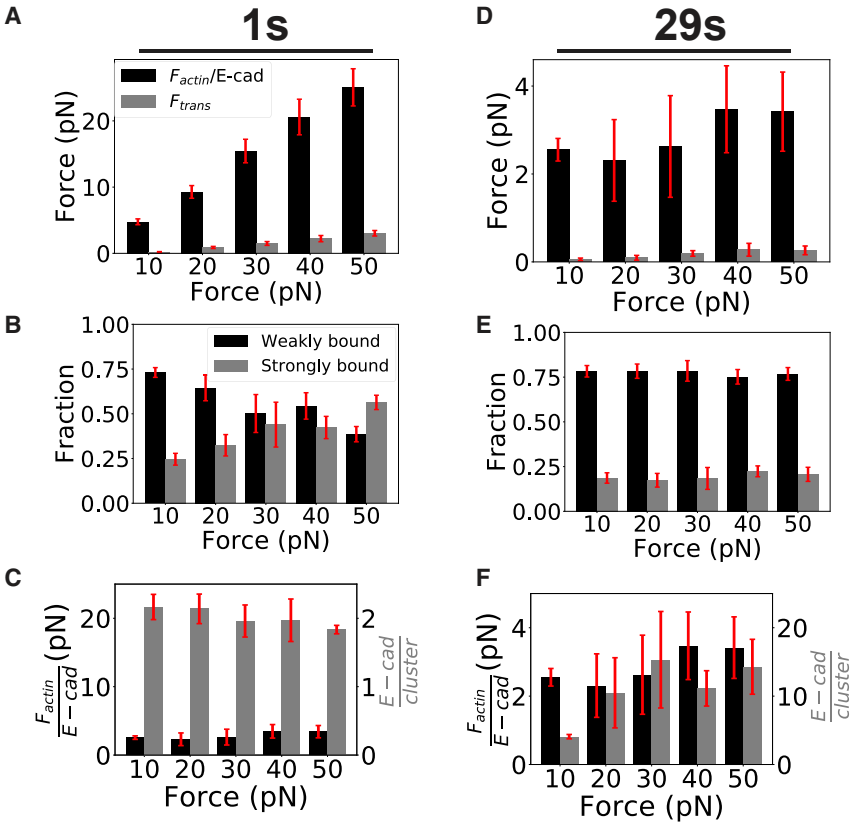

FIGURE 3 Properties of E-cadherin clusters at the beginning of the simulations and at steady state. (*A*) Bar graph showing the average actomyosin force per cluster (*black*) and the transmitted average *trans*-dimer force (*gray*) varying F between 10 and 50 pN, at the beginning of simulations (1 s). (*B*) The fraction of E-cadherins in the strongly and weakly bound states relative to the total number of E-cadherins in *cis*-clusters, varying force from 10 to 50 pN, at the beginning of the simulations (1 s). (*C*) Bar graph showing the average actomyosin force per cluster (*black*) and the average number of E-cadherins per cluster, varying F between 10 and 50 pN, at the beginning of simulations (1 s). (*D–F*) Same measurements as (*A*)–(*C*) at steady state (29 s). All data represent averages from six independent simulations. Error bars are the standard deviation from the mean. To see this figure in color, go online.

magnitude and the time needed for the formation of E-cadherin *cis*-clusters (Fig. 2 *D*). In the first seconds of simulations, the actomyosin force acting on individual clustered dimers is proportional to the cytoskeletal force (Fig. 3 *A*). In the presence of large cytoskeletal force, E-cadherins involved in *cis*-interactions are mostly in the strongly bound state (Fig. 3 *B*), which has long lifetimes (Fig. S1 *B*) and can transmit a significant amount of tension across the dimer. The high tension across the dimer decreases its lifetime (Fig. S1 *A*) and drives it back to the monomer state. As monomers, E-cadherins in a *cis*-cluster have an approximately fourfold higher probability to leave the cluster with respect to other molecular states (Table 1). Therefore, first a fast disassembly of the dimers into monomers occurs within the cluster; then, disconnection of monomers from the cluster occurs under force. These effects result in a higher fraction of free monomers and dimers under force in the first few seconds of simulation (Fig. 2 *C*). At steady state, when nearly constant fractions of E-cadherin molecular states are reached, most dimers have been incorporated into clusters, and the cytoskeletal force acting on individual clustered dimers is small, around 2–4 pN (Fig. 3 *D*), which maintains dimers within clusters. Additionally, dimers in the *cis*-clusters are weakly bound to the actin cytoskeleton at all cytoskeletal force values (Fig. 3 *E*). The weakly bound state presents shorter lifetimes (Fig. S1 *B*) than the strongly bound state and does not transmit a significant amount of tension across the dimers (Fig. 3 *D*), maintaining E-cadherins in the cluster. In sum, stable incorporation of E-cadherins into clusters is slower under increasing cytoskeletal force because an initial fast turnover of E-cadherins in and out of the clusters occurs, followed by stabilization when larger clusters are assembled.

Force increases the size of E-cadherin clusters

Because our model showed that force delays the formation of stable E-cadherin clusters (Fig. 2), we next sought to understand whether force also affects the size of clusters. We first compared the spatial distribution and corresponding molecular states of E-cadherins at 1 s, the onset of clustering, and at 10 s of simulations, when the system reached steady state in terms of fractions of E-cadherin molecular states (Fig. 2). Monomers initially freely diffused and then formed X- and S-dimers and clustered (Fig. 4). In force-free conditions, E-cadherins assembled small clusters that coexisted with free X- and S-dimers at 1 s of simulations (Fig. 4, *left*). Then, a multitude of small sparse spot-like E-cadherin clusters were assembled at 10 s of simulations (Fig. 4, *left*).

Using $F_{actin} = 30$ pN, at 1 s of simulations, a smaller number of clusters formed in comparison to force-free

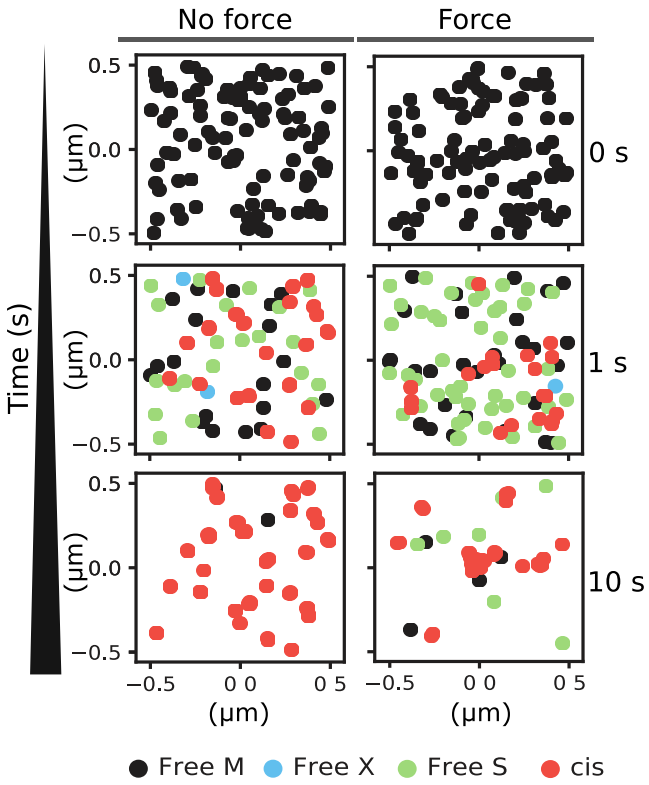

FIGURE 4 Force promotes the formation of large clusters of E-cadherins. Clustering of E-cadherins in force-free conditions (*left*) and under 30 pN cytoskeletal force (*right*). Left: Representative top view of E-cadherin states and positions at the beginning of the simulations (0 s), at the beginning of clustering (1 s), and when the steady state in E-cadherin molecular states is reached (10 s). Right: Representative top view of E-cadherin states and positions at the beginning of the simulations (0 s), at the beginning of clustering (1 s), and when the steady state in E-cadherin molecular states is reached (10 s) under 30 pN force condition. Simulated E-cadherins are single-point particles represented in different colors, depending on their molecular state: black, free monomers; blue, free X-dimers; green, free S-dimers; and red, E-cadherins in *cis*-interactions. To see this figure in color, go online.

conditions (Fig. 4, *right*), and many S-dimers diffused around the clusters (Fig. 4, *right*) because their stable incorporation into the clusters took longer (Fig. 2 *C*). When steady state was reached at 10 s of simulations, large and more concentrated clusters coexisted with a few small ones (Fig. 4, *right*). Cytoskeletal force values of 10 and 50 pN showed similar trends, with a mix of monomers and S-dimers diffusing around smaller *cis*-clusters at 1 s and many free S-dimers around larger clusters at 10 s (Fig. S3, *A* and *B*). Notably, clusters at steady state were consistently larger under force than in force-free conditions. Therefore, these data indicate that force increased the size of E-cadherin clusters at steady state but also enhanced the fraction of diffusive *trans*-dimers (Fig. 4), consistent with trends observed in Fig. 2 *C*. The fraction of S-dimers incorporated in clusters was larger at steady state than at the onset of clustering (Fig. S3, *C* and *D*). At the onset of the simulations, cluster size did not depend on the magnitude of cytoskeletal force (Fig. S2 *C*); however, a direct proportion between cytoskeletal force and cluster size was observed at steady state (Fig. 3 *F*). In our model, cytoskeletal forces above 30 pN decreased the lifetime of both X and S *trans*-dimers (Fig. S1 *A*). At all time points in the simulations, force on clusters was distributed on all E-cadherins of the cluster; therefore, when clusters initially formed and were small (Fig. 3 *C*), E-cadherins were subjected to a large force (Fig. 3 *A*). At steady state, E-cadherins were subjected to a smaller *trans*-dimer force at all cytoskeletal force levels (Fig. 3 *D*). Using high force, E-cadherins in the small clusters that form at the onset of the simulations we subjected to a larger force than E-cadherin in the large clusters emerging at steady state (Fig. 3, *A* and *D*). Accordingly, at 1 s of simulations, individual *trans*-dimers in clusters transmitted up to a few piconewtons of force (Fig. 3 *A*), whereas at steady state, *trans*-dimers transmitted less than 0.2 pN force (Fig. 3 *D*). A high force on small clusters also determined the type of bonds between E-cadherins and actin (Fig. S1 *B*). At a high force, initially strongly bound E-cadherins became weakly bound (Fig. 3, *B* and *E*). Strongly bound E-cadherins often converted into monomers and left the cluster, whereas weakly bound E-cadherins, which could more easily dissociate from actin and therefore not be subjected to force anymore, remained in the cluster, promoting large cluster sizes. In sum, our results indicate that the interplay of force-dependent intracellular and extracellular bond kinetics of E-cadherins result in force-dependent clustering. In particular, they showed that although cytoskeletal force delays clustering (Fig. 2), it promotes the assembly of large clusters and increases the number of freely diffusive *trans*-dimers when steady state is reached (Fig. 4).

Force reduces the density of E-cadherin clusters

Because the results from our simulations showed that actomyosin force promotes the assembly of large clusters while increasing the number of freely diffusive *trans*-dimers (Fig. 4), we next sought to determine how force magnitude affect the number of clusters. By systematically increasing force magnitude, up to 50 pN, and introducing a probability of applying this force to E-cadherins, the fraction of E-cadherins in *cis*-interactions decreased proportionally (Fig. 5 *A*), showing fewer molecules involved in *cis*-interactions. The used probability term models the likelihood that E-cadherins will bind to actin and be subjected to force and can be interpreted as differences in actin architecture and/or myosin activity (45–47). Notably, the proportion of E-cadherins involved in *cis*-interactions was independent of the value of the probability (Fig. 5 *A*), except that clustering became independent of force if this probability was zero, which is expected because E-cadherins were not connected to the cytoskeleton. These results, again, indicate that force can reduce E-cadherin clustering and are consistent with in vivo experiments

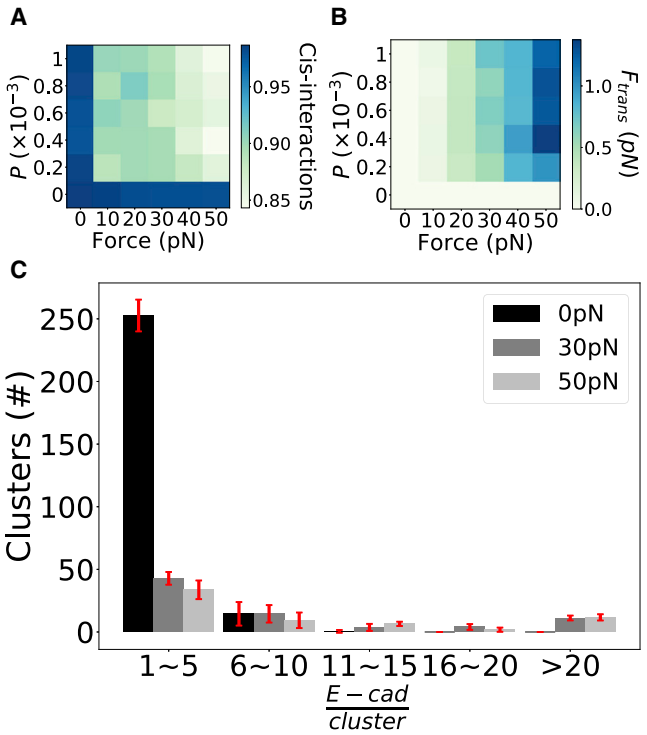

FIGURE 5 Force reduces the numerosity of E-cadherins per unit area. (*A*) Force reduces the fraction of E-cadherins in clusters but increases the size of the clusters. (*A*) Heatmap showing the average proportion of E-cadherins in the *cis* state varying actomyosin force (up to $F_{actin} = 50$ pN) and probability of binding to the actin cytoskeleton, *P*. (*B*) Heatmap of average tension across *trans*-dimers when they are incorporated into *cis*-clusters, varying cytoskeletal force (up to $F_{actin} = 50$ pN) and probability of binding to the cytoskeleton, *P*. All data represent averages from six independent simulations, between 1 and 30 s of simulations. (*C*) Histogram of the average number of clusters versus cluster size under three force conditions: force free (*black*), $F_{actin} = 30$ pN and $p = 0.01$ (*gray*), and $F_{actin} = 50$ pN and $p = 0.01$ (*light gray*). The data are computed from six independent runs, between 10 and 30 s of simulations. Error bars represent the standard deviation from the mean. To see this figure in color, go online.

based on mechanical inference (44). Although the fraction of E-cadherins involved in *cis*-interactions decreased from 0.98 to ~0.8 relative to the total number of E-cadherins, by increasing force magnitude up to 50 pN (Fig. 5 *A*), the force transmitted across *trans*-dimers in the cluster significantly increased, up to ~1.5 pN per E-cadherin (Fig. 5 *B*). In other words, although a smaller fraction of E-cadherins was involved in clusters under increasing force (Fig. 5 *A*), E-cadherins in the clusters transmitted a large force (Fig. 5 *B*). By evaluating the number of clusters with different sizes as a function of force magnitude, our data showed that cluster size increased with force, but cluster number decreased (Fig. 5 *C*). This result did not depend on which cell membrane we analyzed (Fig. S4). Collectively, the results from our model indicate that whereas force destabilizes small clusters and stabilizes large clusters (Fig. 4), it reduces the number of clusters at steady state (Fig. 5 *C*). These differences in cluster size and numerosity under force are consistent with experimental data comparing the sizes of E-cadherin clusters from different sections of lateral cell surfaces, corresponding to differences in force levels (24).

DISCUSSION

The formation of cell-cell adhesions through clustering of E-cadherins is an active process requiring cellular tension (49–51), but how force regulates this mechanism remains largely unknown. To gain insights into clustering of E-cadherins under force, here we developed a computational model based on Brownian dynamics. The model allowed us to evaluate how force governs E-cadherin clustering and the transmission of force across cell-cell adhesions by modulating the molecular states of E-cadherins. Consistent with previous models (31,32,52) and experimental observations (53,54), our model showed that clustering emerges from the cooperation between E-cadherins' adhesive (*trans*-) and lateral (*cis*-) interactions. Additionally, the model showed that cytoskeletal force from binding of E-cadherins to the actomyosin cytoskeleton 1) delays clustering of E-cadherins (Fig. 2 *D*), 2) promotes the formation of large clusters (Fig. 4), and 3) decreases the number of clusters per unit area (Fig. 5 *C*).

Results from the model identify a delay in the assembly of E-cadherin clusters under force (Fig. 2). Without force, sparse puncta-like clusters form, each including few E-cadherin molecules (Fig. 4). Using a small force, clustering of E-cadherins is fast, but the cluster size is small. Using a large force, small clusters are initially destabilized, but once a larger cluster is formed, force promotes its increase in size. This finding is supported by previous in vivo experiments based on mechanical inference, showing an inverse relationship between force and E-cadherin levels in clusters (44). Additionally, cell experiments have demonstrated that different groups of myosin-II exert force on cell surfaces (49) to destabilize E-cadherin *trans*-dimers and thus reduce their ability to form functional adhesion clusters (51). Experiments have also previously detected clusters of different size between the apical part of the cell lateral surface and zonula adherens (55,56). Clusters of larger size and with less intercluster spacing were more likely to appear at the zonula adherens (24), which experiences higher tension than lateral adherens junctions (14,57). Accordingly, with advanced super-resolution microscopy techniques, more concentrated belt-like apical clusters, which are under tension, and spot-like lateral clusters, which are not under tension, were observed in cells (57). The results that force promotes formation of large clusters are also consistent with previous reports showing that E-cadherins play a significant role in the formation of cell-cell adhesions to overcome the surface tangential tension through increased adhesion tension from the expansion of cell-cell contact (58,59).

In the model, binding of E-cadherins to actin occurs when E-cadherins are in clusters, which reproduces α-catenin's activation and binding of actin filaments after nucleation of E-cadherin clusters (14,15,44). Additionally, E-cadherins in the cluster sense and share the mechanical load. Distribution of force across all E-cadherins in the cluster reproduces the linkage of E-cadherins to the actomyosin cytoskeleton through numerous anchors between multiple α-catenins with the same actin filament or bundle (34,35). Binding between α-catenin and actin forms a weak bond at low force, which tends to switch to a stable, strongly bound state at higher force (13). Once initial *cis*-interactions occur between few E-cadherins, the use of a small force generates weak binding between E-cadherin and actin (Fig. 3 *B*), which results in low force transmission (Fig. 5) and distributed puncta-like clusters (Fig. 4). By contrast, using a high force, initially E-cadherins are mostly in the strongly bound state (Fig. 3 *B*), and disassembly of *trans*-interactions can drive E-cadherins away from the clusters. Therefore, initial small clusters tend to be destabilized by force. When these initial clusters reach a dimension that allows for the high actomyosin force to be distributed across many E-cadherins, each E-cadherin can withstand less force and is less likely to leave the cluster. The force-dependent unbinding kinetics of E-cadherin, which underlies their state transitions, generates a "reinforcement" feedback between force and cluster size such that larger clusters emerge under a high force but also take longer to form.

By allowing the tracking of how transitions in molecular state of E-cadherins occur under force and their relation to the emergence of E-cadherin clusters, our model significantly extends previous approaches to cases that better reflect the physiological mechanisms underlying the assembly of cell-cell adhesions. Different from earlier models of cell-cell adhesion assembly (31,32,52), our model explicitly incorporates both extra- and intracellular interactions of E-cadherins, as well as the corresponding force-dependent unbinding kinetics (Fig. S1). The time needed for clustering of E-cadherins is in quantitative agreement with data from micropipette-based measurements of cadherin binding kinetics in live cells (16,60,61). In our model, E-cadherins are represented as explicit point particles that diffuse and transit across structural and functional states to interact with one another and, intracellularly, with the actin cytoskeleton (Fig. 1 *B*). The interaction with the cytoskeleton builds tension on E-cadherins and determines transitions across molecular states, as well as transmission of force across *trans*-dimers. Earlier computational models of E-cadherin clustering used a diffusion-reaction algorithm to simulate cadherin movements and clustering (31). However, in vivo particle tracking experiments have observed different movements of E-cadherins also requiring the actomyosin cytoskeleton (62). Incorporation of actomyosin force, in addition to changing E-cadherin molecular states, reflects E-cadherin motion in and out of clusters, which determines different proportions of clustered E-cadherins at steady state (Fig. 2, *C* and *D*).

To conclude, our mechanistic model of E-cadherin clustering indicates that force modulates the dynamic and steady state properties of E-cadherin clusters by governing transitions across molecular states of individual E-cadherins. Because it incorporates both intracellular and extracellular interactions of E-cadherins, as well as force-dependent mechanisms, our model is a significant extension of previous modeling efforts in adhesion assembly. The results collectively support the general view of a highly dynamic mechanism for E-cadherin adhesion assembly that can be finely tuned by force to ensure tissue homeostasis in physiology and repair in disease.

SUPPORTING MATERIAL

Supporting material can be found online at https://doi.org/10.1016/j.bpj.2021.10.018.

AUTHOR CONTRIBUTIONS

T.C.B. designed the research. Y.C. performed the research. Y.C. analyzed the data. Y.C. and T.C.B. wrote the manuscript. J.B. and O.J.H. edited and revised the manuscript.

ACKNOWLEDGMENTS

We thank Dr. Sanjeevi Sivasankar and Dr. Martijn Gloerich for useful discussion.

This work was supported through the National Science Foundation grant NSF BMMB 2044394 to T.C.B. Computer time was provided by the Scientific Computing and Imaging Institute and the Center for High Performance Computing at the University of Utah.

REFERENCES

1. van Roy, F., and G. Berx. 2008. The cell-cell adhesion molecule E-cadherin. *Cell. Mol. Life Sci.* 65:3756–3788.
2. Liu, Z., J. L. Tan, …, C. S. Chen. 2010. Mechanical tugging force regulates the size of cell-cell junctions. *Proc. Natl. Acad. Sci. USA.* 107:9944–9949.
3. Halbleib, J. M., and W. J. Nelson. 2006. Cadherins in development: cell adhesion, sorting, and tissue morphogenesis. *Genes Dev.* 20:3199–3214.
4. Suffoletto, K., D. Jetta, and S. Z. Hua. 2018. E-cadherin mediated lateral interactions between neighbor cells necessary for collective migration. *J. Biomech.* 71:159–166.
5. Lobos-González, L., L. Aguilar, …, A. F. Quest. 2013. E-cadherin determines Caveolin-1 tumor suppression or metastasis enhancing function in melanoma cells. *Pigment Cell Melanoma Res.* 26:555–570.
6. Liu, X., H. Huang, …, M. A. Hollingsworth. 2014. Loss of E-cadherin and epithelial to mesenchymal transition is not required for cell motility in tissues or for metastasis. *Tissue Barriers.* 2:e969112.
7. Shapiro, L., A. M. Fannon, …, W. A. Hendrickson. 1995. Structural basis of cell-cell adhesion by cadherins. *Nature.* 374:327–337.

8. Patel, S. D., C. Ciatto, …, L. Shapiro. 2006. Type II cadherin ectodomain structures: implications for classical cadherin specificity. *Cell.* 124:1255–1268.
9. Boggon, T. J., J. Murray, …, L. Shapiro. 2002. C-cadherin ectodomain structure and implications for cell adhesion mechanisms. *Science.* 296:1308–1313.
10. Häussinger, D., T. Ahrens, …, S. Grzesiek. 2004. Proteolytic E-cadherin activation followed by solution NMR and X-ray crystallography. *EMBO J.* 23:1699–1708.
11. Thompson, C. J., Z. Su, …, D. K. Schwartz. 2020. Cadherin clusters stabilized by a combination of specific and nonspecific cis-interactions. *eLife.* 9:e59035.
12. Shapiro, L., and W. I. Weis. 2009. Structure and biochemistry of cadherins and catenins. *Cold Spring Harb. Perspect. Biol.* 1:a003053.
13. Buckley, C. D., J. Tan, …, A. R. Dunn. 2014. Cell adhesion. The minimal cadherin-catenin complex binds to actin filaments under force. *Science.* 346:1254211.
14. Biswas, K. H., K. L. Hartman, …, J. T. Groves. 2016. Sustained α-catenin activation at E-cadherin junctions in the absence of mechanical force. *Biophys. J.* 111:1044–1052.
15. Brasch, J., O. J. Harrison, …, L. Shapiro. 2012. Thinking outside the cell: how cadherins drive adhesion. *Trends Cell Biol.* 22:299–310.
16. Chien, Y.-H., N. Jiang, …, D. Leckband. 2008. Two stage cadherin kinetics require multiple extracellular domains but not the cytoplasmic region. *J. Biol. Chem.* 283:1848–1856.
17. Li, Y., N. L. Altorelli, …, A. G. Palmer, III. 2013. Mechanism of E-cadherin dimerization probed by NMR relaxation dispersion. *Proc. Natl. Acad. Sci. USA.* 110:16462–16467.
18. Harrison, O. J., F. Bahna, …, L. Shapiro. 2010. Two-step adhesive binding by classical cadherins. *Nat. Struct. Mol. Biol.* 17:348–357.
19. Meng, W., and M. Takeichi. 2009. Adherens junction: molecular architecture and regulation. *Cold Spring Harb. Perspect. Biol.* 1:a002899.
20. Harrison, O. J., X. Jin, …, B. Honig. 2011. The extracellular architecture of adherens junctions revealed by crystal structures of type I cadherins. *Structure.* 19:244–256.
21. Dustin, M. L., S. K. Bromley, …, C. Zhu. 2001. Identification of self through two-dimensional chemistry and synapses. *Annu. Rev. Cell Dev. Biol.* 17:133–157.
22. Adams, C. L., and W. J. Nelson. 1998. Cytomechanics of cadherin-mediated cell-cell adhesion. *Curr. Opin. Cell Biol.* 10:572–577.
23. Iino, R., I. Koyama, and A. Kusumi. 2001. Single molecule imaging of green fluorescent proteins in living cells: E-cadherin forms oligomers on the free cell surface. *Biophys. J.* 80:2667–2677.
24. Wu, Y., P. Kanchanawong, and R. Zaidel-Bar. 2015. Actin-delimited adhesion-independent clustering of E-cadherin forms the nanoscale building blocks of adherens junctions. *Dev. Cell.* 32:139–154.
25. Thompson, C. J., V. H. Vu, …, D. K. Schwartz. 2019. Cadherin extracellular domain clustering in the absence of *trans*-interactions. *J. Phys. Chem. Lett.* 10:4528–4534.
26. Erami, Z., P. Timpson, …, K. I. Anderson. 2015. There are four dynamically and functionally distinct populations of E-cadherin in cell junctions. *Biol. Open.* 4:1481–1489.
27. le Duc, Q., Q. Shi, …, J. de Rooij. 2010. Vinculin potentiates E-cadherin mechanosensing and is recruited to actin-anchored sites within adherens junctions in a myosin II-dependent manner. *J. Cell Biol.* 189:1107–1115.
28. Borghi, N., M. Sorokina, …, A. R. Dunn. 2012. E-cadherin is under constitutive actomyosin-generated tension that is increased at cell-cell contacts upon externally applied stretch. *Proc. Natl. Acad. Sci. USA.* 109:12568–12573.
29. Sivasankar, S. 2013. Tuning the kinetics of cadherin adhesion. *J. Invest. Dermatol.* 133:2318–2323.
30. Priest, A. V., O. Shafraz, and S. Sivasankar. 2017. Biophysical basis of cadherin mediated cell-cell adhesion. *Exp. Cell Res.* 358:10–13.
31. Chen, J., J. Newhall, …, Y. Wu. 2016. A computational model for kinetic studies of cadherin binding and clustering. *Biophys. J.* 111:1507–1518.
32. Chen, J., Z.-R. Xie, and Y. Wu. 2014. Computational modeling of the interplay between cadherin-mediated cell adhesion and Wnt signaling pathway. *PLoS One.* 9:e100702.
33. Farquhar, M. G., and G. E. Palade. 1965. Cell junctions in amphibian skin. *J. Cell Biol.* 26:263–291.
34. Chen, C.-S., S. Hong, …, S. M. Troyanovsky. 2015. α-Catenin-mediated cadherin clustering couples cadherin and actin dynamics. *J. Cell Biol.* 210:647–661.
35. Maître, J.-L., and C.-P. Heisenberg. 2013. Three functions of cadherins in cell adhesion. *Curr. Biol.* 23:R626–R633.
36. Katsamba, P., K. Carroll, …, B. H. Honig. 2009. Linking molecular affinity and cellular specificity in cadherin-mediated adhesion. *Proc. Natl. Acad. Sci. USA.* 106:11594–11599.
37. Rakshit, S., Y. Zhang, …, S. Sivasankar. 2012. Ideal, catch, and slip bonds in cadherin adhesion. *Proc. Natl. Acad. Sci. USA.* 109:18815–18820.
38. Strale, P.-O., L. Duchesne, …, R. M. Mège. 2015. The formation of ordered nanoclusters controls cadherin anchoring to actin and cell-cell contact fluidity. *J. Cell Biol.* 210:333–346.
39. Baumgartner, W., P. Hinterdorfer, …, D. Drenckhahn. 2000. Cadherin interaction probed by atomic force microscopy. *Proc. Natl. Acad. Sci. USA.* 97:4005–4010.
40. Ganz, A., M. Lambert, …, B. Ladoux. 2006. Traction forces exerted through N-cadherin contacts. *Biol. Cell.* 98:721–730.
41. Pokutta, S., and W. I. Weis. 2000. Structure of the dimerization and beta-catenin-binding region of alpha-catenin. *Mol. Cell.* 5:533–543.
42. Underhill, P. T., and P. S. Doyle. 2004. On the coarse-graining of polymers into bead-spring chains. *J Nonnewton Fluid Mech.* 122:3–31.
43. Shibata-Seki, T., M. Nagaoka, …, T. Akaike. 2020. Direct visualization of the extracellular binding structure of E-cadherins in liquid. *Sci. Rep.* 10:17044.
44. Kale, G. R., X. Yang, …, T. Lecuit. 2018. Distinct contributions of tensile and shear stress on E-cadherin levels during morphogenesis. *Nat. Commun.* 9:5021.
45. Yonemura, S., M. Itoh, …, S. Tsukita. 1995. Cell-to-cell adherens junction formation and actin filament organization: similarities and differences between non-polarized fibroblasts and polarized epithelial cells. *J. Cell Sci.* 108:127–142.
46. Mège, R.-M., J. Gavard, and M. Lambert. 2006. Regulation of cell-cell junctions by the cytoskeleton. *Curr. Opin. Cell Biol.* 18:541–548.
47. Smutny, M., H. L. Cox, …, A. S. Yap. 2010. Myosin II isoforms identify distinct functional modules that support integrity of the epithelial zonula adherens. *Nat. Cell Biol.* 12:696–702.
48. Miyaguchi, K. 2000. Ultrastructure of the zonula adherens revealed by rapid-freeze deep-etching. *J. Struct. Biol.* 132:169–178.
49. Rauzi, M., P.-F. Lenne, and T. Lecuit. 2010. Planar polarized actomyosin contractile flows control epithelial junction remodelling. *Nature.* 468:1110–1114.
50. Collinet, C., M. Rauzi, …, T. Lecuit. 2015. Local and tissue-scale forces drive oriented junction growth during tissue extension. *Nat. Cell Biol.* 17:1247–1258.
51. Chiou, K. K., L. Hufnagel, and B. I. Shraiman. 2012. Mechanical stress inference for two dimensional cell arrays. *PLoS Comput. Biol.* 8:e1002512.
52. Wu, Y., B. Honig, and A. Ben-Shaul. 2013. Theory and simulations of adhesion receptor dimerization on membrane surfaces. *Biophys. J.* 104:1221–1229.
53. Wu, Y., X. Jin, …, A. Ben-Shaul. 2010. Cooperativity between trans and cis interactions in cadherin-mediated junction formation. *Proc. Natl. Acad. Sci. USA.* 107:17592–17597.

54. Wu, Y., J. Vendome, …, B. Honig. 2011. Transforming binding affinities from three dimensions to two with application to cadherin clustering. *Nature.* 475:510–513.

55. Guo, Z., L. J. Neilson, …, R. Zaidel-Bar. 2014. E-cadherin interactome complexity and robustness resolved by quantitative proteomics. *Sci. Signal.* 7:rs7.

56. Wu, S. K., and A. S. Yap. 2013. Patterns in space: coordinating adhesion and actomyosin contractility at E-cadherin junctions. *Cell Commun. Adhes.* 20:201–212.

57. Wu, S. K., G. A. Gomez, …, A. S. Yap. 2014. Cortical F-actin stabilization generates apical-lateral patterns of junctional contractility that integrate cells into epithelia. *Nat. Cell Biol.* 16:167–178.

58. Maître, J.-L., and C.-P. Heisenberg. 2011. The role of adhesion energy in controlling cell-cell contacts. *Curr. Opin. Cell Biol.* 23:508–514.

59. Maître, J.-L., H. Berthoumieux, …, C. P. Heisenberg. 2012. Adhesion functions in cell sorting by mechanically coupling the cortices of adhering cells. *Science.* 338:253–256.

60. Langer, M. D., H. Guo, …, D. E. Leckband. 2012. N-glycosylation alters cadherin-mediated intercellular binding kinetics. *J. Cell Sci.* 125:2478–2485.

61. Chu, Y.-S., W. A. Thomas, …, S. Dufour. 2004. Force measurements in E-cadherin-mediated cell doublets reveal rapid adhesion strengthened by actin cytoskeleton remodeling through Rac and Cdc42. *J. Cell Biol.* 167:1183–1194.

62. Sako, Y., A. Nagafuchi, …, A. Kusumi. 1998. Cytoplasmic regulation of the movement of E-cadherin on the free cell surface as studied by optical tweezers and single particle tracking: corralling and tethering by the membrane skeleton. *J. Cell Biol.* 140:1227–1240.